IEEE P802.15
Wireless Personal Area Networks

Project	IEEE P802.15 Working Group for Wireless Personal Area Networks (WPANs)
Title	**Radio Channel Model for Indoor UWB WPAN Environments**
Date Submitted	[24 June, 2002]
Source	[Jürgen Kunisch, Jörg Pamp] [IMST GmbH] [Carl-Friedrich-Gauß-Str. 2 47475 Kamp-Lintfort Germany] Voice: [+49 2842 981 454] Fax: [+49 2842 981 499] E-mail: [kunisch@imst.de]
Re:	[Call for Contributions on Ultra-wideband Channel Models (02208r1P802-15_SG3a-Call-Contributions-UWB-Channels.doc) 17 April, 2002]
Abstract	[A multipath model based on measurements for the ultra-wideband (UWB) radio channel for WPAN environments is proposed.]
Purpose	[To be used as a reference channel model e.g. for UWB system/link level simulations.]
Notice	This document has been prepared to assist the IEEE P802.15. It is offered as a basis for discussion and is not binding on the contributing individual(s) or organization(s). The material in this document is subject to change in form and content after further study. The contributor(s) reserve(s) the right to add, amend or withdraw material contained herein.
Release	The contributor acknowledges and accepts that this contribution becomes the property of IEEE and may be made publicly available by P802.15.

Scope

This document gives a self-contained specification of a multipath model for the ultra-wideband (UWB) radio channel for WPAN environments which has been designed for link-level simulations. The specification covers both the algorithm and a number of parameter sets for the algorithm which have been derived from radio channel measurements. The focus is put on a concise description of the model rather than its justification (which is to be covered by a separate scientific paper).

The work presented here has partly been funded by the European Commission under contract IST-2000-25197.

Definitions

For the purposes of this document, the following definitions apply:

Individual echo	A single, resolvable echo that is due to a single path, as opposed to dense multipath corresponding to a coherent superposition of many un-resolvable paths.
Multipath cluster height	The maximum ray power expectation value within a given cluster.
Radio channel	An n-port formed by the connectors of transmitting and receiving antennas. In this document $n \equiv 2$.
UWB radio channel	A radio channel that roughly occupies the FCC FR&O 02-48 bands for communications and measurement devices.
Virtual source	A point from which a wave front impinging on the receiver apparently has been emitted if obstruction free propagation is assumed.

References

[1]   FCC, First Report and Order 02-48, Feb. 2002.

[2]   J. Kunisch and J. Pamp, "Measurement results and modeling aspects for the UWB radio channel," *Proc. IEEE UWBST 2002 Conf.*, May 2002.

[3]   J. Kunisch, E. Zollinger, J. Pamp, A. Winkelmann, "MEDIAN 60 GHz wideband indoor radio channel measurements and model," *Proc. IEEE Vehic. Tech. Conf.*, VTC 1999-Fall, pp. 2393-2397.

[4]   A. A. Saleh and R. Valenzuela, "A statistical model for indoor multipath propagation," *IEEE J. Select. Areas Commun.*, vol. SAC-5, pp. 128-137, Feb. 1987.

[5]   D. Cassioli, M. Z. Win, and A. F. Molisch, "A statistical model for the UWB indoor channel," *Proc. IEEE Vehic. Tech. Conf.*, VTC-2001, pp. 1159-1163, 2001.

Introduction

The development of state-of-the-art communications systems typically requires numerical simulations for performance assessments of the envisioned designs. A component which is of paramount importance for reliable results is the channel model used to describe the radio propagation aspect of the system.

Recently, FCC has adopted a First Report and Order to revise Part 15 regarding ultra-wideband transmission systems which puts forth a regulatory frame in the U.S. for UWB systems [1]. In particular, the frequency range specified for communications and measurement systems is 3.1-10.6 GHz.

In this document a radio channel model for indoor UWB environments is proposed that is suitable for WPAN investigations and which covers the above frequency band. The model has been derived from measurements that have been performed in an office environment with line-of-sight, non-line-of-sight, and intermediate conditions for intra-office and inter-office scenarios with omni antennas on both transmitter and receiver side (cf. [2] for a detailed description). The frequency range covered by the measurements is 1 to 11 GHz; the transmitter-receiver separation was below app. 10 m. For a given transmitter position, transfer functions were measured on a rectangular area using a grid of receiver positions with a spacing of 1 cm to achieve spatial oversampling even at the highest frequencies in the band.

As has been pointed out by many researchers, and will be detailed later, a distinguishing feature of the UWB indoor radio channel is that certain *individual* echoes are recognizable and resolvable[1] in the measurements. In contrast to the surrounding dense multipath contributions, these echoes exist individually over distances larger than a wavelength. The model has been designed to reflect this property, i.e. the delay changes of individual echoes corresponding to different spatial positions of the receiver are accounted for to produce a decent Doppler behavior.

The document is organized as follows. Section "Technical Background" discusses some characteristic properties of the UWB channel. The next section "Model Description" gives a narrative description of the model and its elements. In section "Model Summary", the model is compactly presented in an algorithm-like form, whereas the "Constraints, Limitations, and Options" section addresses the general scope of the model. The section on "Implementation Hints" illustrates how central elements of the model may be implemented. Finally, some parameter sets are given in section "Parameter Profiles".

Technical Background

This section briefly discusses some properties which are characteristic for the UWB radio channel. For this document, a property is considered "characteristic" if it is a reasonable requirement for a UWB radio channel model intended for link level simulations to account for these properties, while this may not be necessary for non-UWB models. These properties have been included into the model proposed here.

---

[1] The notion of resolvability is somewhat fuzzy here because the capability to resolve an echo is mostly an attribute of the algorithm used to estimate echo positions, rather than an attribute of the echo itself. An echo may be considered resolvable for example if it can be resolved by an optimal estimator. This in turn poses the problem of what is meant by an "optimal" estimator (e.g. in terms of resolution and accuracy).

The term "ultra-wideband" as used by FCC applies to systems with a fractional bandwidth greater than 0.2, or which occupy more than 500 MHz of spectrum [1]. This definition does not imply a particular frequency band. In this document, a UWB radio channel is understood as a channel with a bandwidth of a few GHz bandwidth, centered around a frequency of a few GHz, roughly within the FCC limits as cited above.

The indoor UWB radio channel differs from the non-UWB radio channel in a number of respects:

Spatial resolution. For indoor environments, the ratio of the spatial resolution (given approximately by the inverse bandwidth) and the characteristic geometric dimensions (e.g. of a room) is such that echoes caused by certain propagation paths may be appreciably distinguishable from each other. This applies in particular to early echoes with small excess delays. For example, in LOS conditions, the direct path, which is first to arrive, may be shorter by more than the spatial resolution (app. 3 cm @ 10 GHz bandwidth) than the path corresponding to the second echo, causing a gap in between these two echoes.

With increasing delay, the arrival probability for paths increases because the corresponding path distances get longer, which in turn increases the probability of interactions with the environment. The result is that interarrival times decrease considerably for increasing delay, and the onset of the inevitable dense multipath contributions is shifted towards larger delays where there are many paths arriving within a resolvable delay duration. For medium to large excess delays, the average power delay profile fits quite well into the exponential decay scheme that has been observed by many researches for frequency-selective non-UWB channels. (cf. e.g. [4]). For small excess delays, however, the UWB channel average power delay profile tends to have a more spiky appearance caused by individual echoes embedded in dense multipath of increasingly lower power. Yet the first path corresponding to LOS conditions may be followed by some trailing multipath contributions caused e.g. by the mechanical antenna support. Depending on the environment and transmitter-receiver distance, the direct path, floor, ceiling and wall reflections may be recognizable.

A typical example for an average power delay profile for a LOS UWB channel illustrating these points is shown in Fig. 1. Fig. 2 shows 150 adjacent color-coded power delay profiles for the same channel over a linear distance of 1.5 m. The individual echoes and the dependence of the corresponding delays from the spatial position (including a slight curvature of the LOS trace due to an appreciable change of the transmitter-receiver distance over the 1.5 m of receiver displacement) are clearly visible. The trace slanted to the right (beginning app. at 13 ns for distance = 0 m) corresponds to a strong wall reflection. Fig. 3 and Fig. 4 show the response of the channel to an impulse with a waveform that corresponds to a Kaiser-Bessel frequency domain window.

Frequency behavior. According to Friis' formula, for ideal antennas with constant effective aperture the free space power gain follows a f^{-2} law (corresponding to an amplitude gain $\sim f^{-1}$), which may be neglected for small fractional bandwidths. For a UWB channel extending from 3 to 11 GHz, however, the f^{-2} law amounts to a difference of app. 11 dB between upper and lower band limits. Strongly depending on the considered environment and the employed antennas, different exponents or other frequency dependencies may occur (cf. [2] for the measurements underlying the model given here). A gain decay with increasing frequency may be expected to cause a reduction of the effective bandwidth as the larger part of the received signal energy concentrates

towards lower frequencies (cf. Fig. 5). To take full advantage of the radio channel (and power spectral density limits) this property has to be considered in both antenna and signal design, and consequently by the channel model.

Model Description

This section gives a general overview of the model and its elements.

Modeled quantity. The basic quantity modeled is the *space-variant baseband impulse response* $h_B(\tau, \vec{r})$, where τ and $\vec{r}$ denote delay and position. From $h_B(\tau, \vec{r})$, a large number of quantities may be derived easily, for example:

- the space-variant baseband transfer function $H_B(f, \vec{r})$ which is the Fourier transform of $h_B(\tau, \vec{r})$ with respect to τ,
- the impulse response $h(\tau, \vec{r}) = \mathrm{Re}(h_B(\tau, \vec{r})\exp(j2\pi F\tau))$, where F is the center frequency,
- the transfer function $H(f, \vec{r})$, which is the Fourier transform of $h(\tau, \vec{r})$ with respect to τ,
- various moments, e.g. r.m.s delay spread, coherence length, etc.

By assuming a certain trajectory $\vec{r}(t)$ of the receiver, space variation may be converted to time variation *as caused by the motion of the receiver*.

From these quantities the received signal corresponding to a certain transmitted impulse waveform may be determined in a straightforward manner by either convolution in delay domain or filtering in frequency domain.

Modeling approach. In the last section it has been pointed out that the average power delay profile basically follows an exponential decay rule. Furthermore, in a dense multipath region, the samples of the baseband impulse response reasonably follow a Rayleigh amplitude statistic [2,3].[2] Therefore the approach put forth in [4] is adopted as a starting point.

In [4], a single multipath cluster is generated by producing echo arrival times according to a homogeneous Poisson process and by drawing echo amplitudes from a Rayleigh distribution with an expectation value that follows an exponential decay law (with a certain decay parameter) as function of echo arrival time. Furthermore, several such clusters are superimposed, where cluster arrival times again are modeled as a homogeneous Poisson process; to each cluster an additional gain applies which follows another exponential decay law based on cluster arrival time. This approach does not, however, reproduce the UWB specific channel behavior for small excess delays. A straightforward modification would consist of changing the homogeneous Poisson process into an inhomogeneous one to model the lower echo arrival probability at low excess delays; unfortunately this approach is not sufficient to cope with the persistence of the individual echoes, i.e. their spatial Doppler behavior.

Instead, the model proposed here is based on the following rules:

---

[2] Note that averaging or integrating the sample *energy* over excess *delay bins* of a certain width may, depending on the mixture of diffuse multipath and individual paths, give rise to a Gamma distribution of the resulting bin energy, i.e., a Nakagami *m*-distribution for the corresponding r.m.s. amplitudes, cf. [5].

- a number of individual echoes (arrival times and complex amplitudes), are generated for several receiver positions $\vec{r}$ according to a certain algorithm described below;
- with each individual echo, a diffuse multipath cluster is associated, with Rayleigh amplitude echoes generated in every bin, an exponential echo power decay law, and uniformly distributed phase;
- the cluster arrival time at position $\vec{r}$ coincides with the arrival time of the associated individual echo at position $\vec{r}$;
- the cluster height (the maximum ray power expectation value within the given cluster) is set to be a certain amount (which is a model parameter) below the power of associated individual echo;
- the decay parameter of each cluster (unique for all clusters) is chosen to have a similar value as the decay parameter of the *overall* single cluster apparent in measurements[3];
- all of these clusters are generated according to the *same* parameters;
- for each individual echo, only a *single* multipath cluster realization is generated, which is used for *all* positions $\vec{r}$;
- for each $\vec{r}$, the individual echoes and their associated clusters are coherently superimposed;

Using a tailored algorithm to generate the arrival times and amplitudes of individual echoes (instead of a homogeneous Poisson process with exponential power decay as in [4]) offers several advantages; in particular the positions of the individual echoes and the associated multipath clusters may be adjusted to render a realistic Doppler spectrum (in wave number domain, corresponding to angle-of-arrival domain) which is consistent with measurement data.

Algorithm for generation of individual echoes. Viewed from the receiver position, and assuming that each individual echo corresponds to a wave front impinging from a certain direction, each of the individual echoes may be thought of as being caused by a wave that was emitted from a *virtual source* situated at a certain distance (the radius of curvature of the wave front) in that direction from the receiver, assuming free space propagation. The proposed model employs this approach and generates a set of virtual sources (see below) from which the parameters of the individual echoes are derived.

Algorithm for generation of virtual sources. It is reasonable to assume that many of the strong low excess delay individual echoes correspond to important low order interactions, e.g. direct transmission and single floor, ceiling, and wall reflections. Therefore, as a first order approximation, positions of potential virtual sources are generated as *image* positions up to a certain order of a given transmitter position in a generic room with respect to given mirror positions. Each wall is assumed to act as a mirror.[4] No other mirrors are considered.

---

[3] Not all UWB indoor radio channels exhibit only a single multipath cluster (cf. [2] for an example) although for the scenarios covered by the parameter profiles given in this document this is the case. Such multi-cluster cases may be covered by the proposed model by a simple and straightforward extension.

[4] This is not to say that all important interactions are specular reflections. The imaging approach is used here because it captures basic characteristic dimensions of generic rooms, and for its algorithmic simplicity.

Model Summary

This section details all of the model equations.
The model parameters are:

Parameter	Dimension	Description
N		Number of samples of h_B in delay domain
R	s^{-1}	Sampling rate in delay domain
B	s^{-1}	Bandwidth of h_B
F	s^{-1}	Center frequency
d_0	m	Reference distance for individual echo power law
α		Path loss exponent for individual echo power law
G_{MP}	dB	Cluster gain with respect to power of associated individual echo
$G_{MP,LOS}$	dB	Additional cluster gain for individual echo corresponding to LOS
G	dB	Basic gain
γ	s	Multipath cluster exponential decay parameter
β		Frequency domain decay exponent
σ_N^2	dB	Normalized noise variance
$x_b(r)$ $y_b(r)$ $z_b(r)$	m	Cartesian coordinates of r-th receiver position
r		Receiver position index
x_t y_t z_t	m	Cartesian coordinates of transmitter position
X_0, X_1 Y_0, Y_1 Z_0, Z_1	m	Mirror positions
Q		Maximum virtual source order per space dimension
$K = \{k\}$		Set of indices of virtual sources to be selected

The following steps are used to generate sampling values $h_B\left(\dfrac{n}{R}, \vec{r}(r)\right)$, $n = 0 \ldots N-1$, of the baseband impulse response:

1. Definition of virtual sources

A grid of virtual source positions is defined by

$$
\begin{aligned}
x_q(m,n,p) &:= \mu(x_t, X_0, X_1, m) \\
y_q(m,n,p) &:= \mu(y_t, Y_0, Y_1, n) \quad \text{for } m,n,p = -Q\ldots Q, \\
z_q(m,n,p) &:= \mu(z_t, Z_0, Z_1, p)
\end{aligned}
\tag{1}
$$

where

$$
\mu(x,a,b,q) := x + q(b-a) + \left(1 - (-1)^q\right)\frac{a+b-2x}{2}.
\tag{2}
$$

This defines a total of $(2Q+1)^3$ virtual sources, which may be numbered from 1 to $(2Q+1)^3$ by a scalar index k according to the correspondence[5]

$$
(m,n,p) \leftrightarrow k = 1 + m + Q + (n+Q)(2Q+1) + (p+Q)(2Q+1)^2.
\tag{3}
$$

To simplify notation, if a single index k is used instead of m, n, p, the correspondence of Eq. (3) is understood.

Note that $(m,n,p) = (0,0,0) \leftrightarrow k = \left((2Q+1)^3 + 1\right)\big/2$ corresponds to the line-of-sight path.

2. Generation of individual echo parameters

From the $(2Q+1)^3$ virtual sources generated above, only $k \in K$ are selected to generate individual echoes. For all $k \in K$ and all receiver position indices r the arrival time (delay) of the k-th individual echo is given by

$$
\tau(k,r) = d(k,r)/c_0
\tag{4}
$$

where $d(k,r)$ is the distance between the k-th virtual source and the r-th receiver position,

$$
d(k,r) = \sqrt{(x_t(k) - x_b(r))^2 + (y_t(k) - y_b(r))^2 + (z_t(k) - z_b(r))^2} \; ;
\tag{5}
$$

the power gain $G(k,r)$ is given by:

If k corresponds to the direct (LOS) path, i.e. $k = \left((2Q+1)^3 + 1\right)\big/2$, then

$$
G(k,r) = \left(\frac{c_0}{4\pi d(k,r)F}\right)^2,
\tag{6}
$$

---

[5] Eq. (3) corresponds to the memory sequence of elements of a multidimensional array with indices m, n, p if the leftmost index (m) counts fastest ("FORTRAN convention").

else[6]

$$G(k,r) = \left(\frac{c_0}{4\pi d_0 F}\right)^2 \left(\frac{d(k,r)}{d_0}\right)^{-\alpha};$$

and the complex amplitude gain is given by

$$A(k,r) = G(k,r)^{1/2} \exp(-j2\pi F\tau(k,r)). \tag{7}$$

3. Generation of associated multipath clusters

For the k-th individual echo, multipath power values

$$|b(k,n)|^2, \quad n = 1\dots N-1, \tag{8}$$

are drawn from an exponential distribution with parameter

$$\mathrm{E}\{|b(k,n)|^2\} = 10^{G_{MP}/10\mathrm{dB}} \exp\left(-\frac{n}{R\gamma}\right), \quad n = 1\dots N-1. \tag{9}$$

If k corresponds to LOS, $G_{MP} + G_{MP,LOS}$ is used instead of G_{MP} in Eq. (9). From theses values, the complex multipath amplitudes (referred to the amplitude of the associated individual echo) follow as

$$b(k,0) := 1,$$

$$b(k,n) = \sqrt{|b(k,n)|^2} \exp(j\phi), \quad n = 1\dots N-1, \tag{10}$$

with a uniform distributed phase ϕ.

4. Superposition of individual echoes and associated multipath clusters

The contribution $h_d(n,r,k)$ of the k-th individual echo and its associated cluster to the normalized baseband impulse response samples $h_d(n,r)$ at receiver position r and delay $\tau(n) = n/R$ is given by

$$h_d(n,r,k) = 10^{G/20\mathrm{dB}} A(k,r) b(k,\mathrm{mod}(n - \lceil R\tau(k,r)\rceil, N)), \quad n = 0\dots N-1. \tag{11}$$

---

[6] Conceptually, the power law is attributed partly to the strength of the virtual source rather than solely to attenuation due to (free space) propagation between the virtual source and the observation point. Assuming a certain power law is equivalent to adopting a certain dependence between virtual source strength and distance to the observation point.

The normalized baseband impulse response samples $h_d(n,r)$ are then given by

$$h_d(n,r) = \sum_{k \in K} h_d(n,r,k).$$

(12)

5. Filtering and frequency power decay

The normalized baseband transfer function $H_d(l,r)$ at receiver position r and baseband frequency $f(l) = \dfrac{R}{N}(\bmod(l + N/2, N) - N/2)$ is obtained by a DFT:

$$H_d(l,r) = \sum_{n=0}^{N-1} h_d(n,r) \exp\left(-j2\pi \frac{nl}{N}\right), \quad l = 0 \dots N-1.$$

(13)

A frequency dependent gain decay and bandwidth limitation is applied by

$$H_d(l,r) \leftarrow H_d(l,r)\left(1 + \frac{f(l)}{F}\right)^{-\beta} \mathrm{rect}\left(\frac{f(l)}{B}\right).$$

(14)

Optionally, at this stage a filter may be applied which corresponds to a different frequency domain window (other than rectangular) or a prescribed transmitted impulse waveform.

6. Noise addition

An inverse DFT of $H_d(l,r)$ yields samples $h_d(n,r)$ of the normalized bandlimited baseband impulse response which may be subjected to observation noise

$$h_d(n,r) \leftarrow h_d(n,r) + s_r(n,r) + js_i(n,r)$$

(15)

where $s_r(n,r)$ and $s_i(n,r)$ are i.i.d. zero mean Gaussian random variables with variance σ_N^2.

7. Normalization

Finally, the relation between $h_d(n,r)$, $H_d(l,r)$ and $h_B(\tau, \vec{r})$, $H_B(f, \vec{r})$ is given by[7]

$$Rh_d(n,r) = h_B\left(\frac{n}{R}, \vec{r}(r)\right), \quad n = 0 \dots N-1,$$

(16)

$$H_d(l,r) = H_B(f(l), \vec{r}(r)), \quad l = 0 \dots N-1,$$

(17)

where $\vec{r}(r) = (x_b(r), y_b(r), z_b(r))^T$. Note that h_B has dimension s^{-1}.

---

[7] Eq. (16) assumes h_B is nonzero only in an interval which is shorter than N/R (no aliasing in delay domain), which implies a constraint for N and R.

Model Scope, Limitations, and Options

The model proposed here is

- basically a statistical model, in the sense that for a model realization certain values are drawn from prescribed distributions with prescribed parameters, and
- it has a minor deterministic component, in the sense that for a model realization certain values (the virtual sources) are derived from a fixed algorithm that does not depend on statistical distributions but on parameters of a trivial surrogate environment.

A computer implementation may thus produce a large number of different realizations of the model. By controlling the seed of the underlying random number generator, this may be done in a reproducible fashion.

Regarding its scope, the model is a

- generic model, in the sense that is does not aim at *predicting* the radio channel for a certain particular environment (e.g. like a ray tracing/imaging based model); instead, it produces results which are similar to *typical* measurement results for certain environments.

The model proposed here is subject to the following limitations:

- For a static transmitter and receiver the model is time-invariant.
- Individual echoes will neither appear nor vanish when $\vec{r}$ varies. This is different to models that use a generation/recombination process (e.g. based on Markov chain approaches).
- Due to the simple algorithm for generation of individual echoes, and due to the subset of measurement data used for model calibration, only small distances of a few meters receiver displacement are reasonably covered by the parameters given in section "Parameter Profiles".

The model offers a number of options for enhancements:

- In this document, the selected echoes are prescribed in the parameter profile. Instead, the selection may be based on various criteria, e.g. minimum/maximum distance, maximum mirroring order, angle-of-arrival and elevation-of-arrival masks, antenna radiation pattern, etc.
- A more general scheme for the power of individual echoes may be introduced.
- Time variance may be introduced by a movement of virtual sources.
- The model is scalable in the sense that by enhancing the complexity of the virtual source determination the model may be shifted towards a more deterministic approach.
- In principle it is possible (by changing the transmitter and receiver coordinates appropriately) to derive matrix channels for $n > 1$ transmitting and $m > 1$ receiving antennas; however, the suitability of the model e.g. for MIMO capacity analysis has not yet been assessed using the measurement data.

Implementation Hints

This section demonstrates how core elements of the model may be implemented in the MATLAB™ programming language [8].

Construction of virtual sources. The following code fragment shows how the grid of virtual sources, the distances to all receiver positions, the echo traces of some selected virtual sources, and the angles of arrival for receiver positions along a distance of 1.5 m may be constructed.

```
% virtual sources
xq          = mirror(1.78, 0, 5.06,   -3:3);
yq          = mirror(4,    0, 5,      -3:3);
zq          = mirror(1.5,  0, 2.75,   -3:3);
[Xq,Yq,Zq]  = ndgrid(xq,yq,zq);

% receiver positions
xb          = 4.5:-.01:3;
yb          = 1.5;
zb          = 1.5;
[Xb,Yb,Zb]  = ndgrid(xb,yb,zb);

% radial distance from each virtual source to each rx position
[XQ,XB]     = ndgrid(Xq,Xb);
[YQ,YB]     = ndgrid(Yq,Yb);
[ZQ,ZB]     = ndgrid(Zq,Zb);
D           = sqrt((XQ-XB).^2+(YQ-YB).^2+(ZQ-ZB).^2);

% indices of selected sources
k           = [172 123 173 130 124 215];

figure(1); clf;
        % plot all virtual source and rx positions
        plot3(Xq(:), Yq(:), Zq(:), 'r.', Xb(:), Yb(:), Zb(:), 'g.');

figure(2); clf;
        % plot echo traces of selected virtual sources
        plot(D(k, : )'/.3, repmat(1:size(D,2),length(k),1)');
        text(D(k,end) /.3, repmat(  size(D,2),length(k),1), num2str(k'));
        xlabel('Delay [ns]');
        ylabel('Distance [cm]');

% azimuth and elevation to virtual source
deg     = pi/180;
A       = atan2(YQ-YB, XQ-XB)/deg;
E       = atan2(ZQ-ZB, sqrt((XQ-XB).^2+(YQ-YB).^2))/deg;

figure(3); clf;
        % plot virtual source elevation vs azimuth for all rx positions
        % and highlight selected virtual sources
        plot(A', E', 'k', A(k,:)', E(k,:)', '.r');
        text(A(k,1), E(k,1), num2str(k'));
        set(gca, 'xdir', 'reverse');
        xlabel('Azimuth [°]');
        ylabel('Elevation [°]');

%-------------------------------------------------------------------------
function x = mirror(x,a,b,q)

x = x + q(:)*(b-a) + (1 - (-1).^q(:))*(a+b-2*x)/2;
```

---

[8] MATLAB™ is a trademark of The Mathworks, Inc. Version ≥ 5 required.

Parameter Profiles

This section gives *preliminary* measurement based parameter profiles for three scenarios:

Profile	Description
Office LOS	Transmission within an office of app. 5 m x 5 m x 2.75 m, line-of-sight condition between transmitter and receiver
Office NLOS	Transmission within an office of app. 5 m x 5 m x 2.75 m, line of sight between transmitter and receiver obstructed by metal cabinet app. 0.6 m x 1.8 m x 2 m
Office-Office	Transmission through light plasterboard wall between two adjacent offices of app. 5 m x 5 m x 2.75 m

Parameter	Unit	Office LOS	Office NLOS	Office-Office
N		2048	2048	2048
R	ns^{-1}	12.8	12.8	12.8
B	GHz	10	10	10
F	GHz	6	6	6
d_0	m	0.8	1.0	3.5
α		3.0	2.0	3.0
G_{MP}	dB	-20.0	-16.0	-19.0
$G_{MP,LOS}$	dB	-13.0	N/A	0.0
G	dB	-5.0	-20.0	-21.0
γ	ns	10.0	9.5	12.5
β		1.1	1.01	1.3
σ_N^2	dB	-118	-123	-121
$x_b(r)$ $y_b(r)$ $z_b(r)$	m	$4.5-0.01r$ $1.5\ (1.5\ldots1.8)$ 1.5	$1.64-0.01r$ $1.5\ (1.5\ldots1.8)$ 1.5	$3.93\ (3.9\ldots4.2)$ $4-0.01r$ 1.5
r		0…150	0…150	0…150
x_t y_t z_t	m	1.78 4 1.5	0.91 4.39 1.5	-1.32 1.8 1.5
X_0, X_1 Y_0, Y_1 Z_0, Z_1	m	0, 5.06 0, 5.00 0, 2.75	0, 5.06 0, 5.12 0, 2.75	-5.06, 5.06 0, 5.12 0, 2.75
Q		3	3	3
$K=\{k\}$		(see below)	(see below)	(see below)

The following tables indicate k, m, n, p, $x_q(m,n,p)/\text{m}$, $y_q(m,n,p)/\text{m}$, $z_q(m,n,p)/\text{m}$, $d(k,0)/\text{m}$, and $\tau(k,0)/\text{ns}$ for the selected virtual sources:

```
OFFICE-LOS
  K     M   N   P       XQ        YQ        ZQ      D(K,0)    T(K,0)

 172    0   0   0     1.780     4.000     1.500     3.035    10.115
 123    0   0  -1     1.780     4.000    -1.500     4.267    14.224
 173    1   0   0     8.340     4.000     1.500     5.448    18.158
 130    0   1  -1     1.780     6.000    -1.500     5.675    18.917
 124    1   0  -1     8.340     4.000    -1.500     6.219    20.730
 215    1  -1   1     8.340    -4.000     4.000     7.741    25.804

OFFICE-NLOS
  K     M   N   P       XQ        YQ        ZQ      D(K,0)    T(K,0)

 171   -1   0   0    -0.910     4.390     1.500     3.854    12.847
 179    0   1   0     0.910     5.850     1.500     4.411    14.703
 164   -1  -1   0    -0.910    -4.390     1.500     6.418    21.394
 115   -1  -1  -1    -0.910    -4.390    -1.500     7.085    23.616
 173    1   0   0     9.210     4.390     1.500     8.103    27.010
 177   -2   1   0    -9.210     5.850     1.500    11.690    38.965

OFFICE-OFFICE
  K     M   N   P       XQ        YQ        ZQ      D(K,0)    T(K,0)

 172    0   0   0    -1.320     1.800     1.500     5.692    18.974
 221    0   0   1    -1.320     1.800     4.000     6.217    20.724
 123    0   0  -1    -1.320     1.800    -1.500     6.434    21.448
 179    0   1   0    -1.320     8.440     1.500     6.876    22.919
 228    0   1   1    -1.320     8.440     4.000     7.316    24.387
 130    0   1  -1    -1.320     8.440    -1.500     7.502    25.006
 173    1   0   0    11.440     1.800     1.500     7.826    26.085
  32    0   1  -3    -1.320     8.440    -7.000    10.933    36.443
 312    0  -1   3    -1.320    -1.800     9.500    11.189    37.298
 110    1  -2  -1    11.440    -8.440    -1.500    14.838    49.459
 174    2   0   0    18.920     1.800     1.500    15.151    50.502
 170   -2   0   0   -21.560     1.800     1.500    25.585    85.283
```
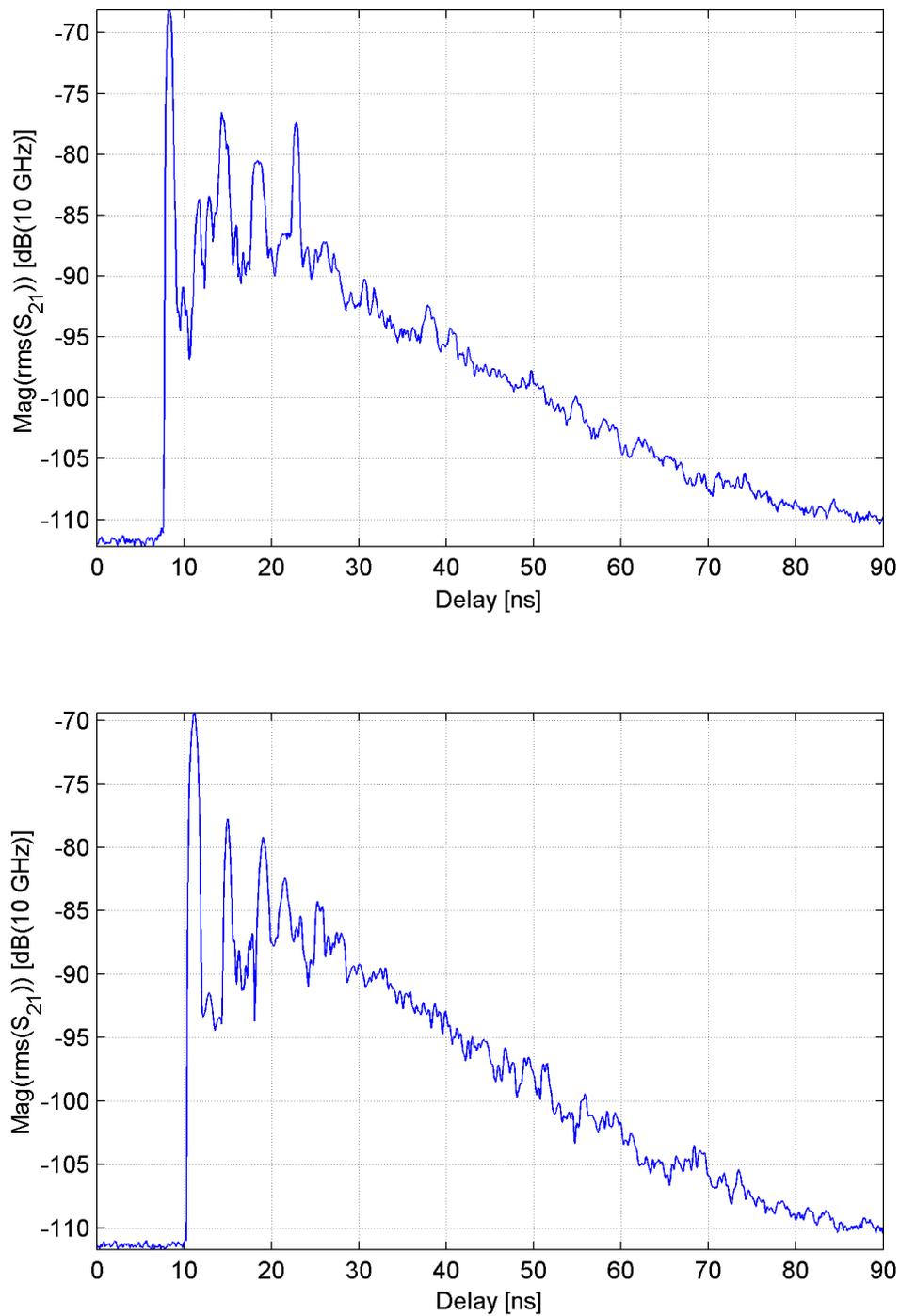
Fig. 1. Average power delay profile for 30 x 30 baseband impulse responses on a 30 cm x 30 cm grid for LOS conditions. Top: measurement, bottom: model.
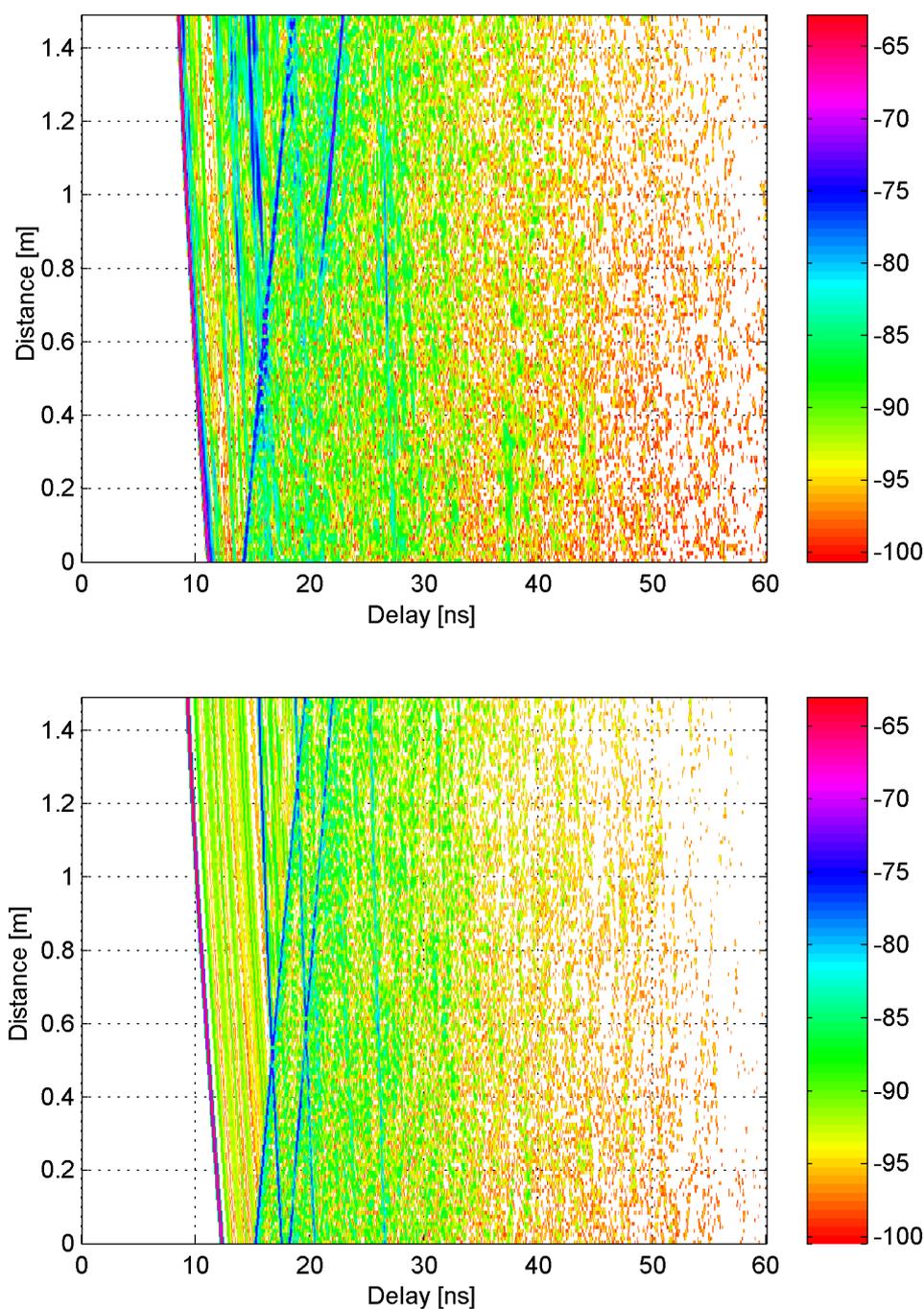
Fig. 2. Color-coded power delay profiles for 150 baseband impulse responses along 150 cm distance almost perpendicular to the Rx-Tx line-of-sight. Top: measurement, bottom: model.
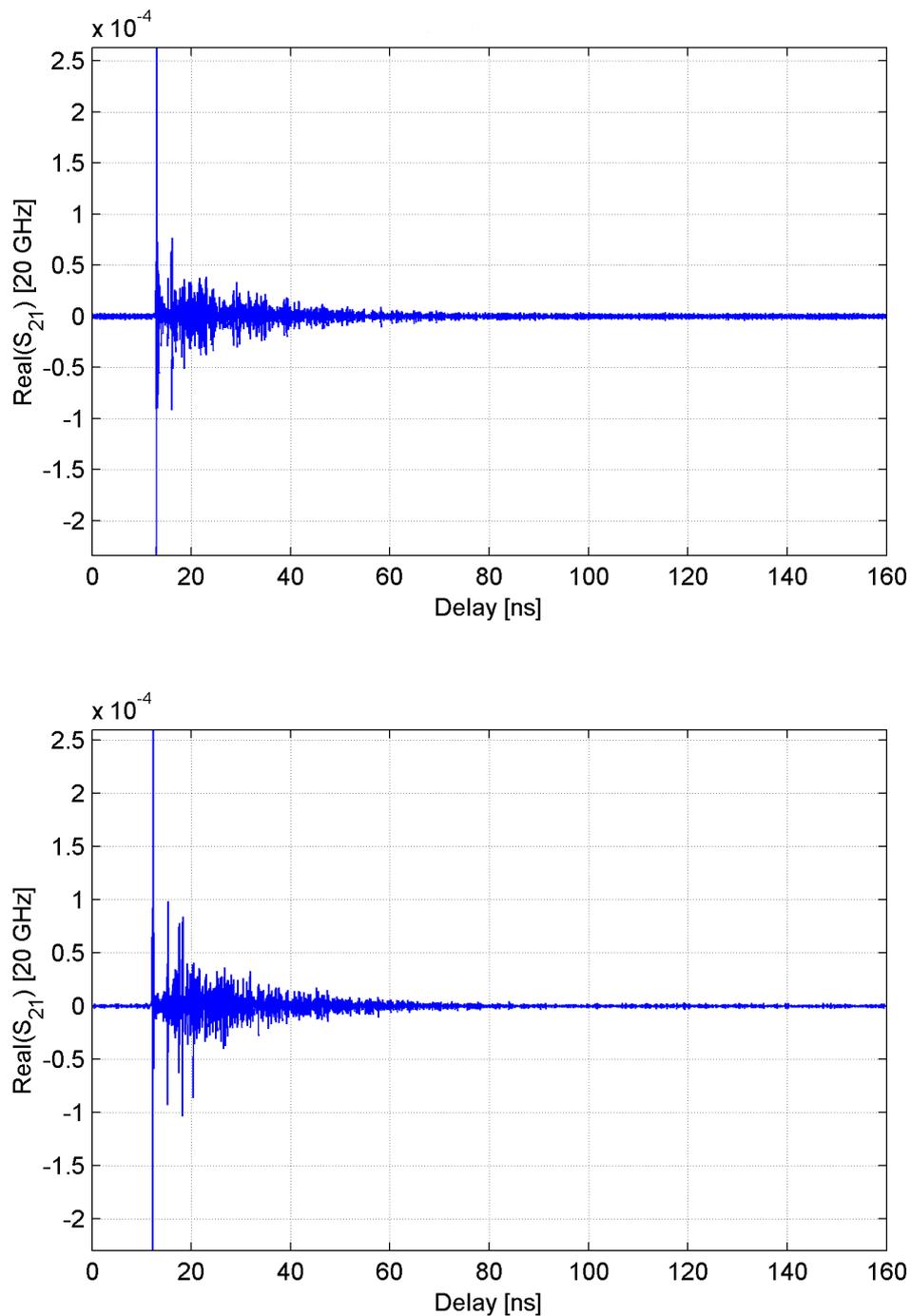
Fig. 3. Example for a single impulse response. Top: measurement, bottom: model. A Kaiser-Bessel frequency domain window has been applied.
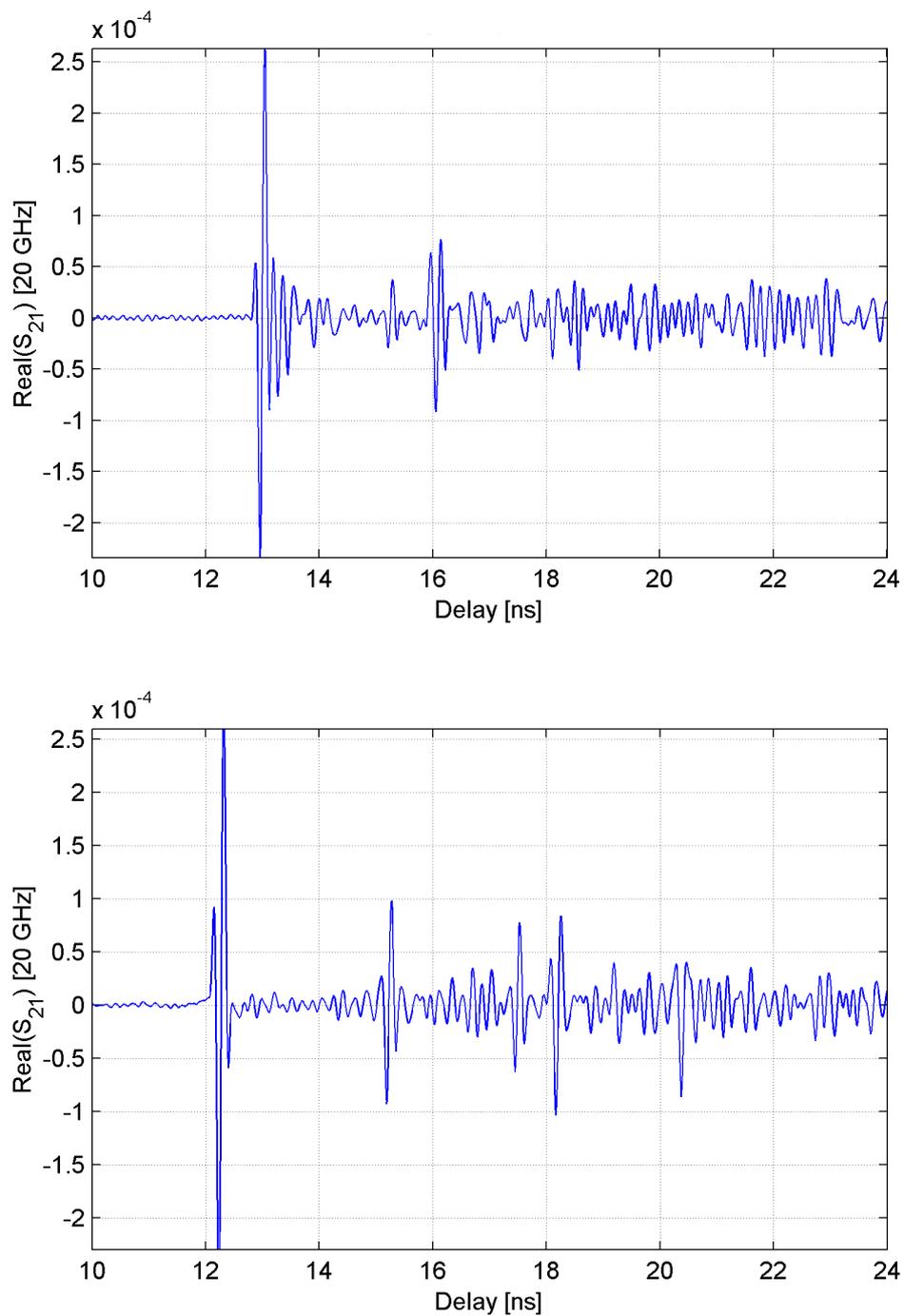
Fig. 4. Example for a single impulse response (initial 10 ns of excess delay). Top: measurement, bottom: model. A Kaiser-Bessel frequency domain window has been applied.
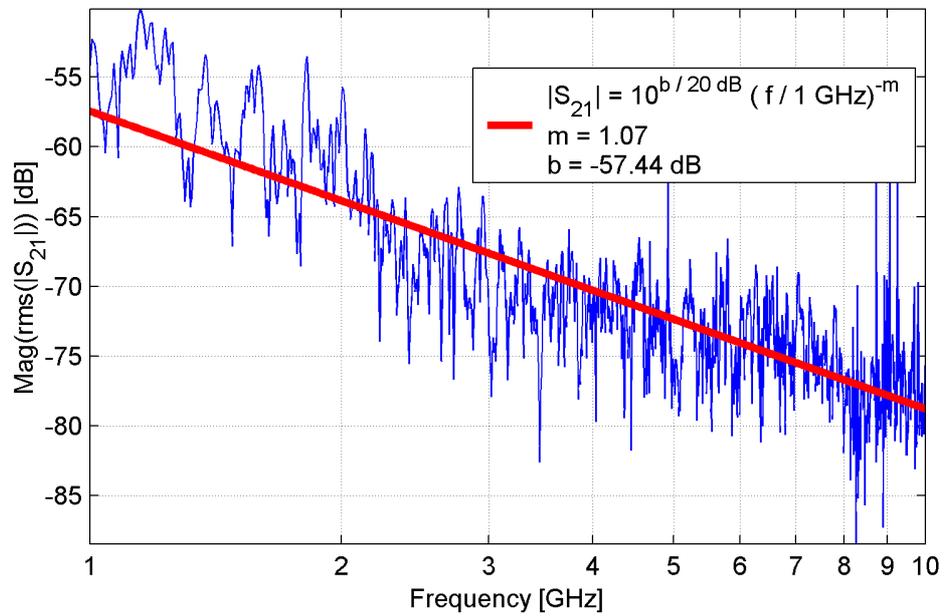
Fig. 5. Example for decay of channel gain with frequency (r.m.s. average of 10 measured transfer functions for non-LOS conditions).